Dynamic Response of Prevacuolar Compartments to Brefeldin A in Plant Cells[1][W][OA]

Yu Chung Tse, Sze Wan Lo, Stefan Hillmer, Paul Dupree, and Liwen Jiang*

Department of Biology (Y.C.T., S.W.L., L.J.) and Molecular Biotechnology Program (Y.C.T., S.W.L., L.J.), The Chinese University of Hong Kong, Shatin, New Territories, Hong Kong, China; Department of Cell Biology, Heidelberg Institute for Plant Sciences, University of Heidelberg, D–69120 Heidelberg, Germany (S.H.); and Department of Biochemistry, University of Cambridge, Cambridge CB2 1QW, United Kingdom (P.D.)

Little is known about the dynamics and molecular components of plant prevacuolar compartments (PVCs) in the secretory pathway. Using transgenic tobacco (*Nicotiana tabacum*) Bright-Yellow-2 (BY-2) cells expressing membrane-anchored yellow fluorescent protein (YFP) reporters marking Golgi or PVCs, we have recently demonstrated that PVCs are mobile multivesicular bodies defined by vacuolar sorting receptor proteins. Here, we demonstrate that Golgi and PVCs have different sensitivity in response to brefeldin A (BFA) treatment in living tobacco BY-2 cells. BFA at low concentrations (5–10 μg mL^{-1}) induced YFP-marked Golgi stacks to form both endoplasmic reticulum-Golgi hybrid structures and BFA-induced aggregates, but had little effect on YFP-marked PVCs in transgenic BY-2 cells at both confocal and immunogold electron microscopy levels. However, BFA at high concentrations (50–100 μg mL^{-1}) caused both YFP-marked Golgi stacks and PVCs to form aggregates in a dose- and time-dependent manner. Normal Golgi or PVC signals can be recovered upon removal of BFA from the culture media. Confocal immunofluorescence and immunogold electron microscopy studies with specific organelle markers further demonstrate that the PVC aggregates are distinct, but physically associated, with Golgi aggregates in BFA-treated cells and that PVCs might lose their internal vesicle structures at high BFA concentration. In addition, vacuolar sorting receptor-marked PVCs in root-tip cells of tobacco, pea (*Pisum sativum*), mung bean (*Vigna radiata*), and Arabidopsis (*Arabidopsis thaliana*) upon BFA treatment are also induced to form similar aggregates. Thus, we have demonstrated that the effects of BFA are not limited to endoplasmic reticulum and Golgi, but extend to PVC in the endomembrane system, which might provide a quick tool for distinguishing Golgi from PVC for its identification and characterization, as well as a possible new tool in studying PVC-mediated protein traffic in plant cells.

All eukaryotic cells have secretory and endocytic pathways that are composed of several functionally distinct membrane-bound compartments, each with characteristic proteins that can be used as markers to define these compartments. Prevacuolar compartments (PVCs) or late endosomes are intermediate organelles where secretory and endocytic traffic leads to vacuole or lysosome merge (Bethke and Jones, 2000; Lemmon and Traub, 2000; Jiang and Rogers, 2003; Maxfield and McGraw, 2004; Lam et al., 2005). These prevacuolar or late endosomal compartments characteristically possess internal microvesicles and are thus called multivesicular bodies (MVBs) or endosomes. In animal cells, these microvesicles appear to originate in the early or recycling endosomes (Parton et al., 1992) and have a different protein composition to the limiting membrane (Griffiths et al., 1990; Kobayashi et al., 1998). The microvesicles and the soluble content of these MVBs are most likely delivered into the interior of the lysosomal compartment via direct fusion (Luzio et al., 2000; Katzmann et al., 2002).

In spite of the obviously important role of PVCs in mediating protein traffic to vacuoles in the secretory and endocytic pathways, the identification and characterization of plant PVCs, both functionally and morphologically, have been challenging due to the complexity of the plant vacuolar system, the existence of multiple transport pathways leading to distinct vacuoles, and the lack of good markers (antibody and reporter) to be used to define or identify PVCs (Jiang and Rogers, 1998, 2003; Bethke and Jones, 2000; Lam et al., 2005). Putative plant PVCs were identified using antibodies specific for the Arabidopsis (*Arabidopsis thaliana*) syntaxin Pep12p and the pea (*Pisum sativum*) vacuolar sorting receptor (VSR) BP-80 (Bassham et al., 1995; Conceicao et al., 1997; Paris et al., 1997). Studies on the relative distribution of VSR proteins between Golgi stacks and PVCs in various plant cells demonstrated that VSR proteins largely separated from Golgi markers and thus must be concentrated on PVCs under steady-state conditions (Li et al., 2002). In addition, a chimeric BP-80 reporter containing the BP-80 transmembrane domain and cytoplasmic tail colocalized

[1] This work was supported by the Research Grants Council of Hong Kong (grant nos. CUHK4156/01M, CUHK4260/02M, CUHK4307/03M, and CUHK4580/05M), the National Science Foundation of China (grant no. 30529001), and the Chinese University of Hong Kong Scheme C (to L.J.).

* Corresponding author; e-mail ljiang@cuhk.edu.hk; fax 852–2603–5646.

The author responsible for distribution of materials integral to the findings presented in this article in accordance with the policy described in the Instructions for Authors (www.plantphysiol.org) is: Liwen Jiang (ljiang@cuhk.edu.hk).

[W] The online version of this article contains Web-only data.

[OA] Open Access articles can be viewed online without a subscription.

www.plantphysiol.org/cgi/doi/10.1104/pp.106.090423

with endogenous VSR proteins when the reporter was expressed in transgenic tobacco (*Nicotiana tabacum*) culture cells (Jiang and Rogers, 1998). Therefore, both VSR proteins and the BP-80 reporter can be used as markers to define and identify plant PVCs.

MVB-type organelles have been described some time ago in plant cells (Robinson et al., 2000). Typically, MVBs in plant cells are somewhat smaller than a Golgi stack and have an osmiophilic plaque somewhere on their surface, a feature shared by multivesicular endosomes in mammalian cells (Raposo et al., 2001; van Dam and Stoorvogel, 2002). Conclusive proof that plant PVCs are MVBs was provided by a recent study (Tse et al., 2004) that demonstrated the presence of VSR proteins in MVBs by immunogold labeling of tobacco Bright-Yellow-2 (BY-2) cell sections, where VSR labeling was restricted to the boundary membrane rather than the internal vesicles of the MVBs, suggesting that only a small proportion of the VSRs that reach the PVC at any one time are destined for degradation. Further confirmation that MVBs are PVCs and are distinct from Golgi stacks comes from examining the differential effects of the drug wortmannin. Whereas wortmannin at reversible concentrations (10–30 μM) primarily causes MVBs to vacuolate and lose their osmiophilic plaques, it leads to a reduction in the number of internal vesicles as well (Tse et al., 2004). These changes have also been recorded for multivesicular endosomes in mammalian cells (Bright et al., 2001; Sachse et al., 2002). Thus, wortmannin appears to be a useful MVB/PVC-specific drug and is becoming a very useful tool for perturbing transport to the lytic vacuole in plant cells (daSilva et al., 2005).

Similar to wortmannin, the fungal macrocyclic lactone brefeldin A (BFA) has been widely used in studying protein trafficking in the secretory and endocytic pathways of eukaryotic cells. In mammalian cells, BFA targets a subclass of Sec7-type guanine nucleotide exchange factors (GEFs) required for converting the GDP ribosylation factor 1 (Arf1p) to its GTP form (Jackson and Casanova, 2000), which then binds to the membrane to recruit coatomer and leads to the production of coatomer protein (COPI)-coated vesicles, whereas, BFA disrupts the formation of COPI-coated vesicles by inhibiting the conversion of the Arf1p from its GDP form to a GTP form by locking the reaction intermediate in an inactive complex. Plant cells may have a similar molecular target to BFA. For example, the Arabidopsis gene GNOM encoding an Arf GEF has been identified (Busch et al., 1996) and localized to the Golgi apparatus (Jackson and Casanova, 2000). In addition, the rapid release of COPI from the Golgi stacks into the cytosol was also demonstrated in tobacco BY-2 cells using anti-Atγ-COPI antibodies in confocal immunofluorescence (Ritzenthaler et al., 2002).

The Golgi apparatus is likely the initial site in response to BFA in both plant and mammalian cells (Sciaky et al., 1997; Nebenfuhr et al., 2002). In addition to blocking protein transport from the endoplasmic reticulum (ER) to the Golgi, BFA at low concentrations (2–10 μg mL^{-1}) also leads to rapid and dramatic changes in the morphology of the Golgi apparatus of mammalian cells, where the Golgi apparatus gets extensively tubulated and fuses with the ER (Klausner et al., 1992). In addition, BFA may also act on endosomes and induce endosomes to become tubulated in mammalian cells (Hunziker et al., 1991; Lippincott-Schwartz et al., 1991; Wood et al., 1991). In plant cells, BFA also induced the Golgi apparatus to form ER-Golgi hybrid structures (Ritzenthaler et al., 2002), BFA compartments (Satiat-Jeunemaitre et al., 1996; Wee et al., 1998; Baldwin et al., 2001; Tse et al., 2004), or the loss of Golgi cis-cisternae (Hess et al., 2000). In addition, BFA may induce the trans-Golgi network to incorporate into BFA compartments in Arabidopsis root cells (Dettmer et al., 2006). Moreover, some studies also demonstrated that BFA (at 25–50 μM mL^{-1}) induces endosomal compartments from aggregates in Arabidopsis root cells (Geldner et al., 2003; Grebe et al., 2003). However, little is known about the possible effects of BFA on PVCs/MVBs in the secretory pathway of plant cells.

We previously demonstrated that VSR proteins can be used as markers to define plant PVCs (Li et al., 2002). Recently, we developed two transgenic BY-2 cell lines expressing the Golgi marker GONST1-yellow fluorescent protein (YFP) reporter and the PVC marker YFP BP-80 reporter and demonstrated that the YFP BP-80 reporter and VSR proteins defined PVCs with characteristics of MVBs in BY-2 cells (Tse et al., 2004). In addition, BFA at a concentration of $<$10 μg mL^{-1} induced the YFP-marked Golgi stacks, but not the YFP-marked PVCs, to form enlarged compartments in transgenic BY-2 cells. Therefore, these transgenic BY-2 cells are useful tools in studying the dynamics of the Golgi and PVCs in response to external stimuli in living cells.

In this study, we extended our understanding of BFA effects on PVCs/MVBs in plant cells. We used these two transgenic BY-2 cell lines expressing YFP/green fluorescent protein (GFP) reporters marking Golgi and PVC to test the hypothesis that BFA also affects other endomembrane organelles in addition to the ER and the Golgi apparatus. Here, we demonstrated that YFP-marked PVC and YFP-marked Golgi stacks showed different sensitivity in response to BFA treatment. BFA at low concentrations (5–10 μg mL^{-1}) induced YFP-marked Golgi stacks, but not YFP-marked PVC, to form aggregates. However, BFA at higher concentrations (50 or 100 μg mL^{-1}) induced both YFP-marked PVC and Golgi stacks to form typical enlarged structures in a dose- and time-dependent manner. Confocal immunofluorescence studies demonstrated that BFA-induced aggregates derived from YFP-marked PVCs colocalized with VSR proteins, but kept physically distinct from the Golgi-derived aggregates in BFA-treated cells. Further immunogold electron microscopy (immunoEM) and structural EM studies identified unique structures of Golgi- and PVC-derived aggregates. In addition, BFA also induced VSR-marked PVCs to form similar aggregates in root tip cells of pea, tobacco, mung bean (*Vigna radiata*), and Arabidopsis.

RESULTS

Development of the GFP BP-80 Transgenic Cell Line

We have previously demonstrated that VSR proteins are markers for defining PVCs in plant cells (Li et al., 2002). More recently, we have developed two transgenic tobacco BY-2 cell lines expressing the Golgi reporter GONST1-YFP and the PVC reporter YFP BP-80 and demonstrated that these two reporters colocalized with ManI and VSR antibodies, respectively (Tse et al., 2004). We further demonstrated that PVCs in tobacco BY-2 cells are MVBs that are marked by VSR proteins (Tse et al., 2004).

As a first step to compare reporter-marked Golgi to PVC directly in transgenic living tobacco BY-2 cells, we further developed a new transgenic tobacco BY-2 cell line expressing the GFP BP-80 fusion in which the GFP was used to replace the YFP in the previous YFP BP-80 construct (Tse et al., 2004). Similar to the transgenic cell line expressing the Golgi marker GONST1-YFP (Fig. 1A, image 1), typical punctate fluorescent signals were detected from cells expressing the GFP BP-80 (Fig. 1A, image 2). Furthermore, organelles marked by either YFP BP-80 or GFP BP-80 were mostly (more than 92% based on calculation from more than 20 labeled cells) colocalized with VSR antibodies (Fig. 1A, images 3 and 4), indicating PVC localization of both YFP BP-80 and GFP BP-80 in transgenic tobacco BY-2 cells.

Golgi localization of the GONST1-YFP reporter and PVC localization of the GFP/YFP BP-80 reporter in transgenic BY-2 cells were further confirmed by immunoEM studies where GFP antibodies specifically labeled Golgi stacks (Fig. 1B, left image) or MVB (Fig. 1B, right image) in transgenic BY-2 cells expressing either Golgi or PVC reporters. Thus, similar to YFP BP-80, the GFP BP-80 reporter served as a tool for defining PVCs/MVBs in tobacco BY-2 cells. Therefore, from now on, both YFP BP-80 and GFP BP-80 cell lines were used as PVC markers in this study.

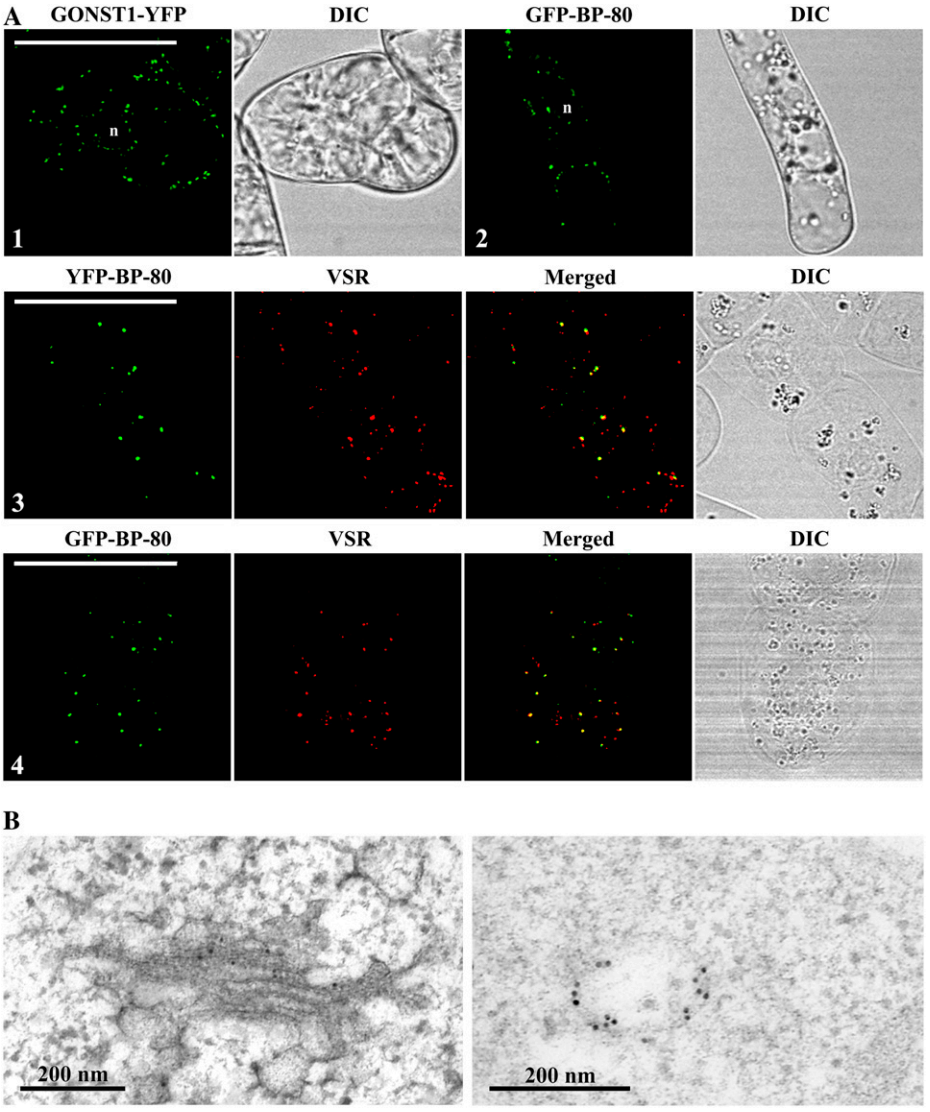

Figure 1. Subcellular localization of two reporters in transgenic BY-2 cells. A, Confocal immunofluorescent study of reporters. Similar punctate signals were detected from transgenic BY-2 cells expressing either the Golgi marker GONST1-YFP (image 1) or the PVC marker GFP-BP-80 (image 2), where both YFP BP-80 and GFP BP-80 reporter (green) largely colocalized with VSR antibodies (red). DIC images show the morphology of the tested cells. n, Nucleus. Bars = 50 μm. B, ImmunoEM localization of GONST1-YFP and GFP BP-80. Ultrathin sections prepared from high-pressure frozen/freeze-substituted transgenic GONST1-YFP BY-2 cells were labeled with either GFP antibodies (left) to detect the Golgi-localized GONST1-YFP reporter or VSR antibodies (right) to detect multivesicular PVCs. Bars = 200 nm.

PVC and Golgi Have Different Sensitivity to BFA

BFA has been a useful tool in studying protein trafficking in the secretory pathway because this drug induced Golgi stacks to form enlarged compartments and prevented protein traffic from the ER to the Golgi (Jiang and Rogers, 1998; Hess et al., 2000; Ritzenthaler et al., 2002). Using transgenic tobacco BY-2 cell lines expressing Golgi and PVC reporters, we have recently demonstrated that Golgi and PVC had different sensitivity to wortmannin in which the drug induced the PVC, but not the Golgi, to dilate (Tse et al., 2004). Because the Golgi and PVC are closely related organelles in the secretory pathway using transgenic BY-2 cell lines expressing PVC reporters, we therefore wanted to study the possible effects of BFA on PVCs. As a control, a transgenic cell line expressing the Golgi reporter was used.

We first performed a dose-response experiment in which day 3 transgenic cell lines expressing either the Golgi or PVC reporters were incubated with various concentrations of BFA (from 0–100 μg mL^{-1}) for 1 h before the treated cells were collected and used in confocal imaging. Day 3 BY-2 cells have been used in our drug treatment studies because these cells are at their log phase (Matsuoka et al., 2004) and XFP BP-80 fusions remain in PVCs as punctate patterns, which will be targeted to vacuoles as diffusion patterns at day 6 and day 7 (Mitsuhashi et al., 2000; Lo and Jiang, 2006). As shown in Figure 2, in cells expressing the Golgi marker GONST1-YFP, typical enlarged compartments were observed in all cells treated with BFA at tested concentrations from 5 μg mL^{-1} to 100 μg mL^{-1} (Fig. 2A, arrows) and the average sizes of the visible BFA-induced aggregates were larger in cells treated with higher concentrations of BFA (Fig. 2C). To our surprise, in cells expressing the PVC marker YFP BP-80, BFA at high concentrations (50–100 μg mL^{-1}) also induced the YFP-marked PVCs to form similar aggregates (Fig. 2, B [arrows] and C), even though low BFA concentrations (5–10 μg mL^{-1}) did not have any visible effect on the size and number of YFP-marked PVCs (Fig. 2, C and D). Similar results were obtained when cells were treated with BFA with various concentrations for 2 h before confocal imaging (Supplemental Fig. S1). In addition, similar results were also obtained when another transgenic cell line expressing the PVC marker GFP BP-80 was used in a similar study (data not shown).

BFA at 5 to10 μg mL^{-1} induced the GONST1-YFP-marked Golgi to form aggregates in transgenic BY-2 cells (Fig. 2A); this result is consistent with several previous studies showing BFA-induced Golgi aggregation in different cell types (Wee et al., 1998; Baldwin et al., 2001; Tse et al., 2004; Miao et al., 2006). However, several other studies showed that BFA at such concentrations also induced GFP-marked Golgi to form ER patterns in both BY-2 and tobacco leaf cells (Ritzenthaler et al., 2002; Saint-Jore et al., 2002). To find out the possible causes for such observed differences, we collected BY-2 cells at day 3 and day 6 for BFA treatment at 10 μg mL^{-1} for 1 h before confocal imaging. Day 3 and day 6 cells represent the log phase and the stationary phase, respectively (Matsuoka et al., 2004). As shown in Supplemental Figure S2, similar punctate patterns were observed in GONST1-YFP cells collected at either day 3 or day 6 (left images 1 and 6). At the end of 1-h BFA treatment, major aggregation patterns were observed from day 3 cells (left images 2 and 3) or day 2 cells (data not shown), but typical ER patterns were observed from BFA-treated day 6 cells (left images 5 and 6) or day 7 cells (data not shown), indicating that the physiological status of GONST1-YFP BY-2 cells may affect its responsive patterns to BFA treatment. However, when the same BFA treatments were performed using transgenic Man1-GFP BY-2 cells, ER patterns were observed from both BFA-treated day 3 (right images 2 and 3) and day 6 cells (right images 5 and 6). We do not know whether such observed differences are due to the difference between the trans-Golgi GONST1 and the cis-Golgi Man1 or to the different cell line used, but such differences shall not affect this study on the effects of BFA on PVCs/MVBs, where the GONST1-YFP cells were used as a control for XFP BP-80-marked PVC/MVBs in BY-2 cells (see ''Discussion'').

To study further the dynamics of the BFA-induced response of PVCs to high concentrations of BFA, a time-course study was carried out using these two transgenic cell lines. Day 3 individual transgenic cell lines were first incubated with BFA at 50 μg mL^{-1}, a minimal concentration that induced PVCs to form aggregates (Fig. 2), followed by sample collection at indicated times after BFA treatment for confocal imaging. As shown in Figure 3A, in cells expressing the Golgi marker GONST1-YFP, enlarged BFA-induced aggregates were already detected 15 min after BFA treatment and these aggregated structures remained throughout the 2-h period of BFA treatment. In contrast, in cells expressing the PVC marker YFP BP-80, no BFA-induced YFP-marked aggregates were detected (Fig. 3, B and C) and the number of YFP-marked PVCs remained unchanged (Fig. 3D) during the first 30 min of BFA treatment, but similar aggregates were observed from 45 min after BFA treatment and these aggregates remained detectable thereafter for 2 h (Fig. 3, B and C). Thus, when comparing to Golgi stacks, a 30-min delay was observed for PVCs to form BFA-induced aggregates in response to BFA at 50 μg mL^{-1} under these conditions.

Recovery of PVCs from BFA Treatment

Low concentrations of BFA (typically between 5 and 10 μg mL^{-1}) have been commonly used in studying protein trafficking and organelle dynamics in tobacco BY-2 cells (Nebenfuhr et al., 2002). In cells treated with BFA at this low concentration, the normal Golgi apparatus can usually recover upon removal of the drug from the culture medium. It is thus believed that the

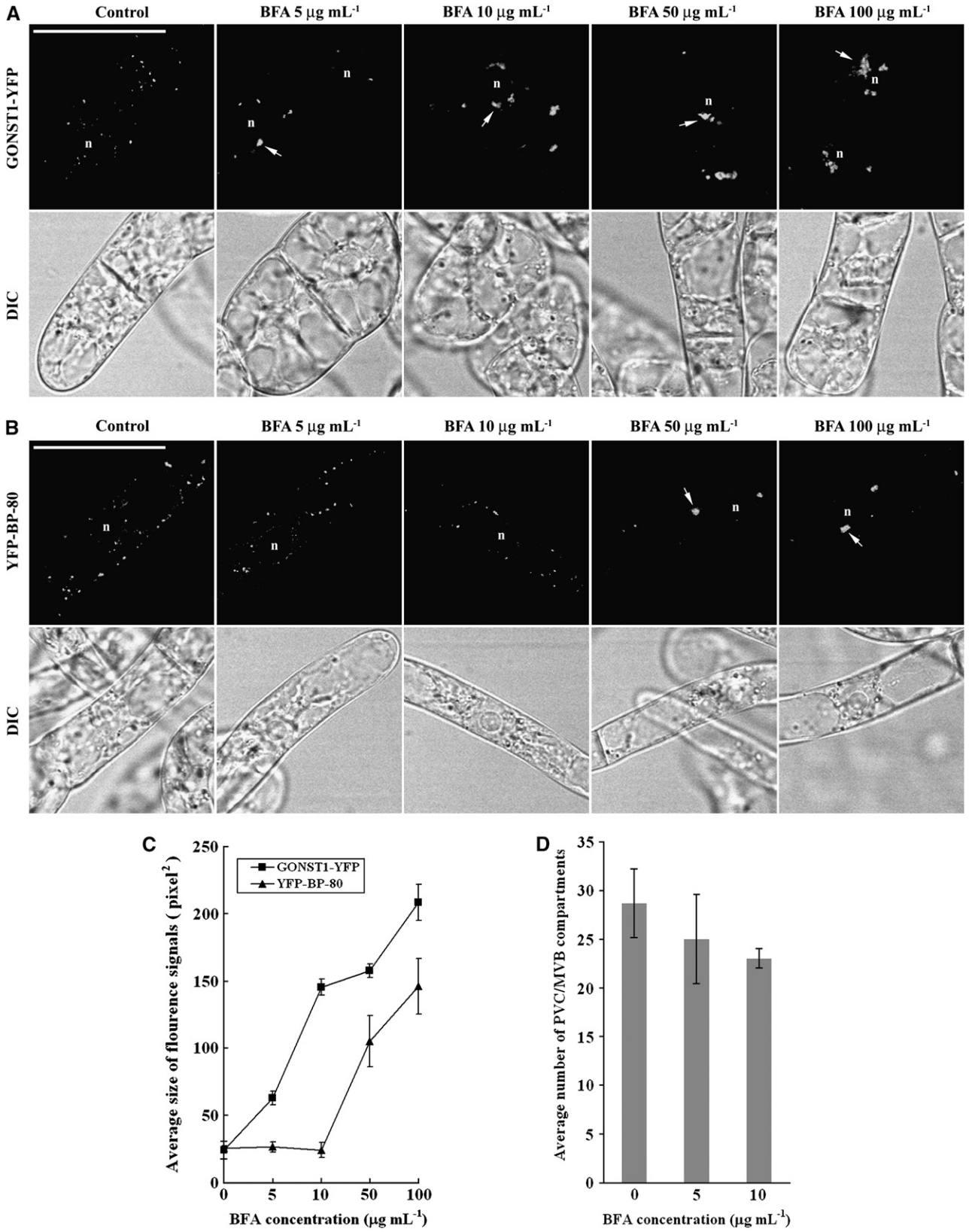

Figure 2. BFA induces YFP-marked PVCs to form aggregates in a dose-dependent manner. A and B, Transgenic BY-2 cells expressing either the Golgi marker GONST1-YFP (A) or the PVC marker YFP BP-80 (B) were incubated with BFA at various concentrations, as indicated, for 1 h before they were collected for confocal imaging of YFP signals. Arrows indicate examples of

formation of BFA-induced compartments and ER-Golgi hybrids is not caused by the toxic effect of BFA on BY-2 cells.

To find out whether BFA at 50 or 100 μg mL^{-1} is toxic to BY-2 cells and causes permanent damage, we performed a recovery study. Day 3 transgenic cells expressing the Golgi marker GONST1-YFP and PVC marker GFP BP-80 were treated with BFA at 100 μg mL^{-1} for 1 h, followed by washing off the BFA with fresh medium and then sampling collections at indicated time points upon recovery for confocal imaging. As shown in Figure 4A, in cells expressing the Golgi marker GONST1-YFP, fluorescent signals in both aggregates and an ER pattern were detected 15 and 45 min after BFA washing, which was then followed by disappearance of aggregates, reappearance of punctate signals, and weakening of the ER pattern after 1 h, and a fully punctate pattern was eventually observed after 2 h (Fig. 4A). These results indicate that the Golgi pattern can be recovered fully upon BFA removal. Similar patterns of changes were also detected in cells expressing the PVC marker GFP BP-80 upon removal of BFA and, again, normal punctate signals were recovered after 2 h (Fig. 4B). Furthermore, the BFA-treated BY-2 cells during the recovery period still looked normal as judged by their appearance in the differential interference contrast (DIC) images. Similar results were obtained when cells were treated with BFA at 50 μg mL^{-1} for 1 h, followed by washing off BFA in the recovery study in these two cell lines (Supplemental Fig. S3). These results demonstrate that BFA at 50 or 100 μg mL^{-1} did not permanently damage the treated BY-2 cells and that the BFA-induced aggregates from either Golgi or PVC organelles can be fully recovered into typical punctate patterns upon removal of BFA. Therefore, both Golgi apparatus and PVCs in transgenic BY-2 cells demonstrated the ability of recovery even in high doses of BFA treatment at 50 or 100 μg mL^{-1}.

BFA-Induced Compartments Derived from Golgi and PVC Remain Distinct, But Are Closely Associated

BFA at 5 to 10 μg mL^{-1} induced formation of aggregates that may represent ER-Golgi hybrid structures in BY-2 cells (Ritzenthaler et al., 2002). Our results thus far indicated that BFA at 50 or 100 μg mL^{-1} induced both Golgi apparatus and PVCs to form aggregates in transgenic BY-2 cells. Because both YFP-marked Golgi and PVC exhibit similar punctate patterns before BFA treatment and form similar aggregates in the presence of BFA, it is thus possible that the BFA-induced aggregates were derived from Golgi and PVC fusion.

To find out whether BFA-induced aggregates derived from Golgi and PVC remain distinct or fusion upon BFA treatment, we performed the following immunofluorescent labeling study. Day 3 transgenic BY-2 cells expressing GONST1-YFP and YFP BP-80 reporters were treated with BFA at 50 μg mL^{-1} for 1 and 2 h, followed by fixation and labeled with VSR antibodies for subsequent confocal imaging. As shown in Figure 5, the PVC/MVB marker VSR antibodies detected aggregates (red) in fixed transgenic cells expressing either the Golgi or PVC reporter (Fig. 5). Interestingly, in fixed transgenic BY-2 cells expressing the PVC marker YFP BP-80, the BFA-induced aggregates derived from the YFP-marked PVCs (green) colocalized (more than 90%) with aggregates detected by VSR antibodies (red; Fig. 5, image 1, arrowheads in merged image). In contrast, in fixed BY-2 cells expressing the Golgi marker GONST1-YFP, BFA-induced aggregates derived from the GONST1-YFP-marked Golgi (green) remained largely distinct (more than 90%) from the aggregates marked by the PVC marker VSR antibodies (red) at 1 or 2 h after BFA treatment (Fig. 5 images 2 and 3, arrowhead versus arrow in merged images). In addition, most of these aggregates derived from Golgi and PVC showed close association and tended to join together. These results demonstrate that BFA-induced aggregates derived from Golgi stacks are different from those derived from PVCs in BY-2 cells and that VSR proteins remain intact within the PVC-derived aggregates in BY-2 cells.

To further investigate the nature and relationship of BFA-induced aggregates derived from Golgi and PVC in response to BFA treatment, we then performed a time-course experiment using transgenic cells expressing the Golgi marker GONST1-YFP. These transgenic cells were first incubated with BFA at 50 μg mL^{-1}, followed by sample collection and fixation at an indicated time point before the fixed cells were used in labeling with VSR antibodies for subsequent confocal imaging analysis. As shown in Figure 6, BFA-induced aggregates marked by the Golgi marker GONST1-YFP (green) were already detected 10 min after BFA treatment, and these aggregates remained similar throughout the 2-h treatment period (Fig. 6, images 1–3; green). In contrast, the VSR-marked PVCs (red) remained unchanged during the first 10 min, whereas VSR-marked aggregates became visible and gradually increased in 2 h (Fig. 6, images 1–3; red). In addition, aggregates derived from Golgi and PVC remained distinct, but closely associated (Fig. 6, merged images 2 and 3). The differential response of Golgi and PVC to BFA treatment was consistent with results obtained from living cells (Figs. 2 and 3).

Figure 2. (*Continued.*)
BFA-induced aggregates in cells expressing these two reporters. DIC images show the morphology of the tested cells. n, Nucleus. Bars = 50 μm. C, Average sizes of the fluorescence signals of GONST1-YFP and YFP BP-80 in transgenic BY-2 cells treated with BFA at 50 μg mL^{-1} at indicated times (calculated using image J software on images of 500 $\times$ 500 pixels with 200 dpi). D, Average numbers of YFP BP-80-marked PVCs in transgenic BY-2 cells treated with BFA at indicated concentrations (0, 5, and 10 μg/mL) for 1 h.

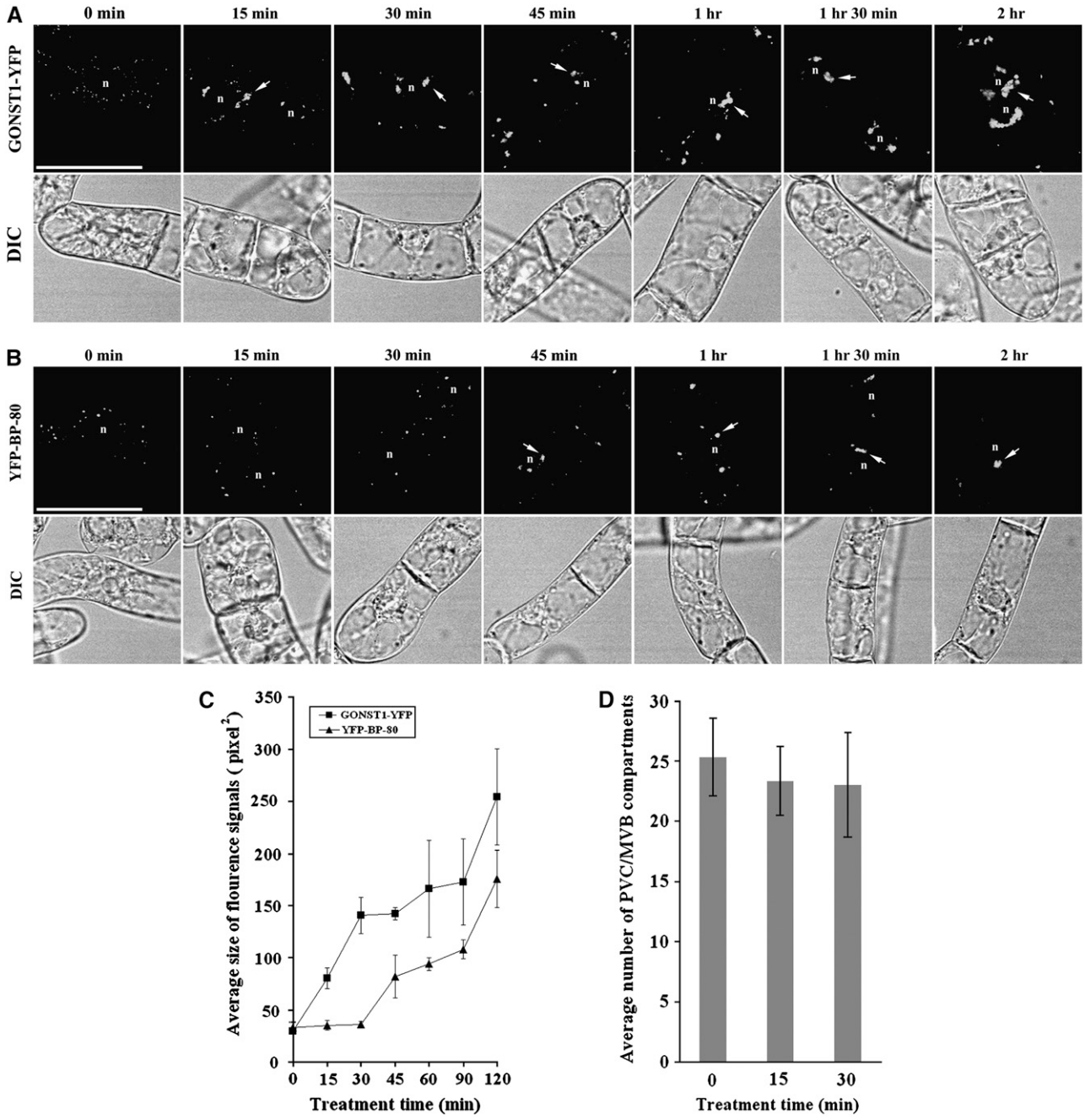

Figure 3. Time-course formation of BFA-induced Golgi or PVC aggregates. A and B, Transgenic BY-2 cells expressing the Golgi marker GONST1-YFP (A) and the PVC marker YFP BP-80 (B) were first incubated with BFA at 50 μg mL^{-1}, followed by sample collection at indicated times for confocal imaging of YFP signals. Arrows indicate examples of BFA-induced aggregates derived from either the YFP-marked Golgi (A) or the YFP-marked PVCs (B). DIC images show the morphology of the tested cells. n, Nucleus. Bars = 50 μm. C, Average sizes of the fluorescence signals of GONST1-YFP and YFP BP-80 in transgenic BY-2 cells treated with BFA at 50 μg mL^{-1} at indicated times (calculated using imageJ software on images of 500 $\times$ 500 pixels with 200 dpi). D, Average numbers of YFP BP-80-marked PVCs in a single transgenic BY-2 cell at indicated times upon BFA treatment at 50 μg/mL.

BFA Effects on the Golgi and PVC Are Pharmacologically Distinguishable

To find out whether the effect of BFA on the formation of PVC-derived aggregates is a primary effect on a PVC target or a secondary effect of transport from the Golgi to the PVC, we performed the following experiments using two phospholipase A_2 inhibitors, ONO-RS-082 and bromoenol lactone (BEL), which have been used to inhibit the effect of BFA in mammalian cells (de Figueiredo et al., 1998, 1999). In addition, ONO in mammalian cells targets and disrupts the Golgi

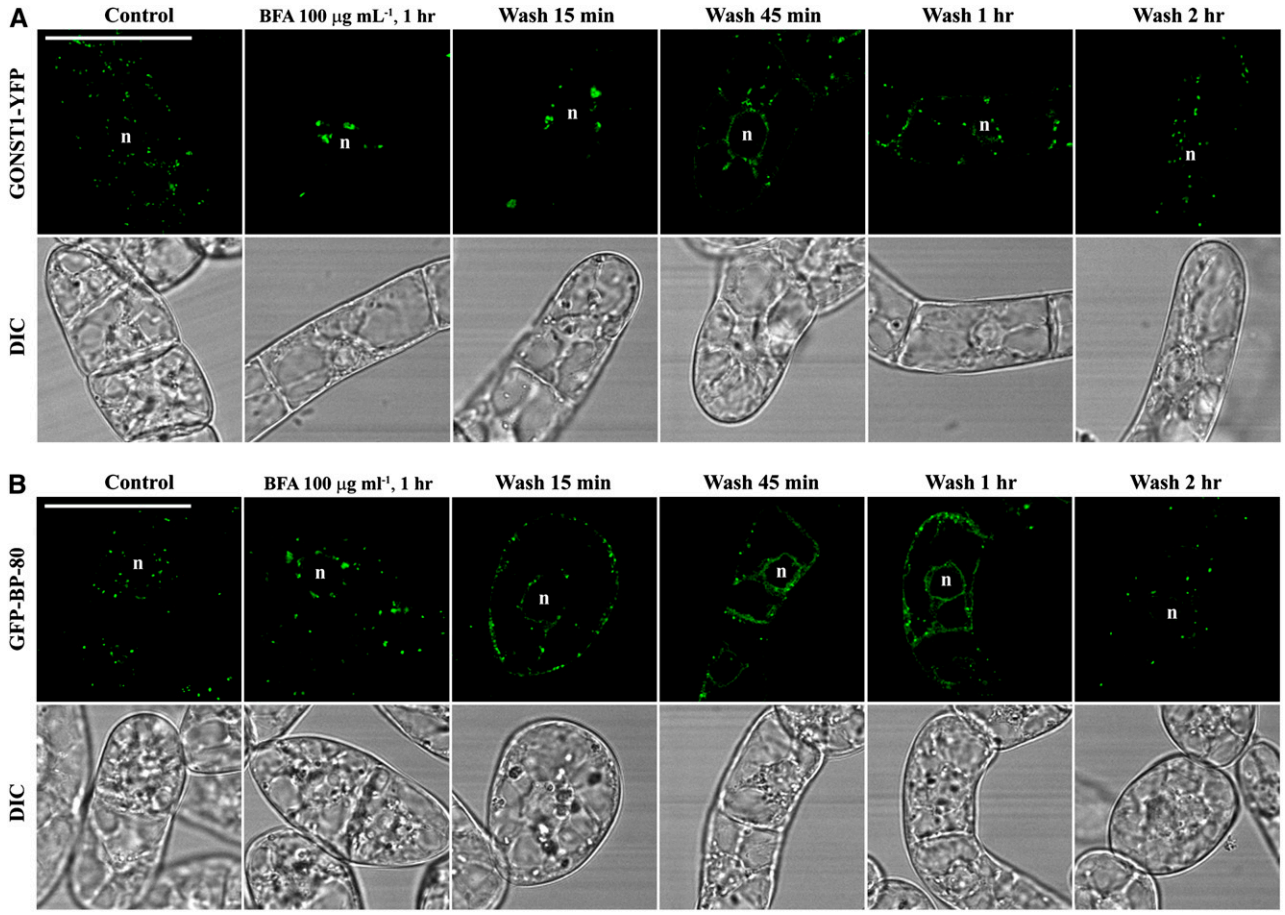

Figure 4. Recovery of BFA-induced aggregates. Transgenic BY-2 cells expressing the Golgi marker GONST1-YFP (A) and the PVC marker GFP BP-80 (B) were treated with BFA at 100 μg mL^{-1} for 1 h before BFA was washed off with fresh Murashige and Skoog medium, followed by sample collection at indicated times for confocal imaging. DIC images show the morphology of the tested cells. n, Nucleus. Bars = 50 μm.

apparatus (de Figueiredo et al., 1999). Transgenic BY-2 cells expressing the Golgi marker GONST1-YFP were pretreated with ONO-RS-082 at 10 μM for 15 min, followed by addition of BFA at 10 or 100 μg mL^{-1} for an additional hour before confocal imaging. As shown in Figure 7, BFA at either 10 or 100 μg mL^{-1} induced the GNOST1-YFP-marked Golgi to form aggregates in cells without pretreatment with ONO-RS-082 (Fig. 7A, images 1 and 2). Similar aggregates were observed in cells pretreated with ONO-RS-082 at 10 μM for 15 min followed by BFA treatment at either 10 or 100 μg mL^{-1} (Fig. 7A, images 3 and 4), indicating that this drug did not block the BFA effect on Golgi at either low or high concentrations. However, in transgenic BY-2 cells expressing the PVC marker GFP BP-80, BFA at 100 μg mL^{-1} induced the GFP-marked PVC to form aggregates in cells without pretreatment with ONO-RS-082 (Fig. 7A, image 2), but no such aggregates were observed in cells pretreated with ONO-RS-082 at 10 μM for 15 min (Fig. 7A, image 4), indicating that the drug prevents the formation of BFA-induced PVC aggregates. When a similar drug, BEL, was used to pretreat cells before BFA treatment at 100 μg mL^{-1}, it did not block the formation of BFA-induced aggregates from Golgi or PVC (Supplemental Fig. S4), indicating that ONO-RS-082 was specific for PVC. These results clearly demonstrated that BFA acts on different targets on the Golgi and the PVC; whereas ONO-RS-082 did not prevent the formation of BFA-induced aggregates from the Golgi, the drug blocked the formation of BFA-induced PVC aggregates. Therefore, it is likely that BFA acts on distinct targets on Golgi and PVC, respectively, even though its molecular mechanism of actions on Golgi and PVC remained to be illustrated in plant cells.

Morphology of BFA-Induced Golgi and PVC Aggregates

Confocal immunofluorescent studies thus far demonstrate that BFA at high concentration (50–100 μg mL^{-1}) induced both Golgi and PVC to form aggregates that are closely adjacent to each other. To further identify and study the morphological structures of these BFA-induced aggregates and their relationship, immunoEM studies were then carried out where GFP and VSR antibodies were used to detect Golgi stacks

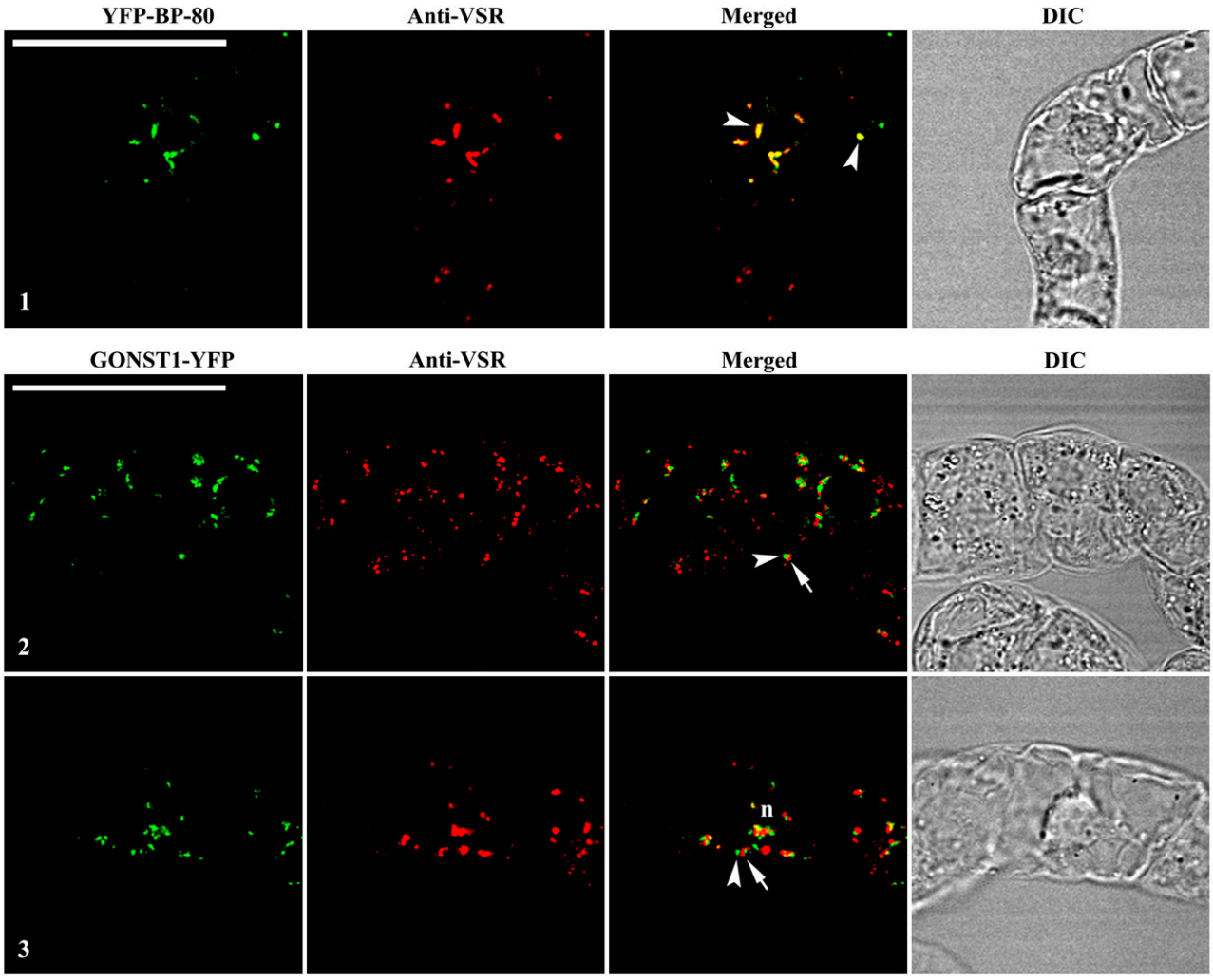

Figure 5. BFA-induced PVC aggregates are distinct from Golgi aggregates. Transgenic BY-2 cells expressing the Golgi marker GONST1-YFP and the PVC marker YFP BP-80 were treated with BFA at 50 μg mL^{-1} for 1 h (images 1 and 2) or 2 h (image 3) prior to fixation. The fixed cells were then labeled with VSR antibodies to detect PVCs (red), whereas the YFP reporters (green) were ready for detection. Arrowheads in merged image 1 indicate examples of colocalization between the PVC reporter YFP BP-80 and VSR antibodies. Arrowheads and arrows in images 2 and 3 indicate examples of distinct, but closely associated, BFA-induced aggregates derived from Golgi (green) and PVC (red; termed Golgi-PVC hybrid). DIC images show the morphology of the tested cells. Bars = 50 μm.

and PVCs, respectively, in transgenic GONST1-YFP BY-2 cells. Day 3 GONST1-YFP transgenic BY-2 cells were treated with BFA at 100 μg mL^{-1} for 1 h before they were fixed by glutaraldehyde and embedded in Lowicryl (HM20). Ultrathin sections were then prepared for immunoEM labeling. As shown in Figure 8, normal Golgi apparatus (Fig. 8A) was specifically labeled by GFP antibodies in untreated control cells. In contrast, in BFA-treated cells, curved Golgi aggregates were labeled specifically by GFP antibodies (Fig. 8B), which may likely represent the BFA-induced aggregates derived from the Golgi apparatus.

Because no visible MVBs were detected in ultrathin sections prepared from Lowicryl (HM20) blocks, we therefore prepared samples using a high-pressure frozen/freeze substituted protocol for immunoEM studies (Tse et al., 2004). As shown in Figure 8, in the untreated control cells, multivesicular PVCs were clearly labeled by VSR antibodies and labeling was mainly on the peripheral regions (Fig. 8, C and D). Similarly, in BFA-treated cells, similar sizes (100–200 nm) of vesicles were also labeled specifically by VSR antibodies to their peripheral membranes (Fig. 8, E–H). Moreover, unlike untreated cells where PVC/MVBs were often identified individually, these VSR-labeled vesicles were often detected as groups that tended to pack together and thus might be derived from PVC aggregation or vesiculation (Fig. 8, E–I). However, these aggregated vesicles containing VSR proteins seem to lose their MVB appearance because no visible internal vesicles were detected from these VSR-labeled PVCs under these conditions (see, for example, Fig. 8, E and G).

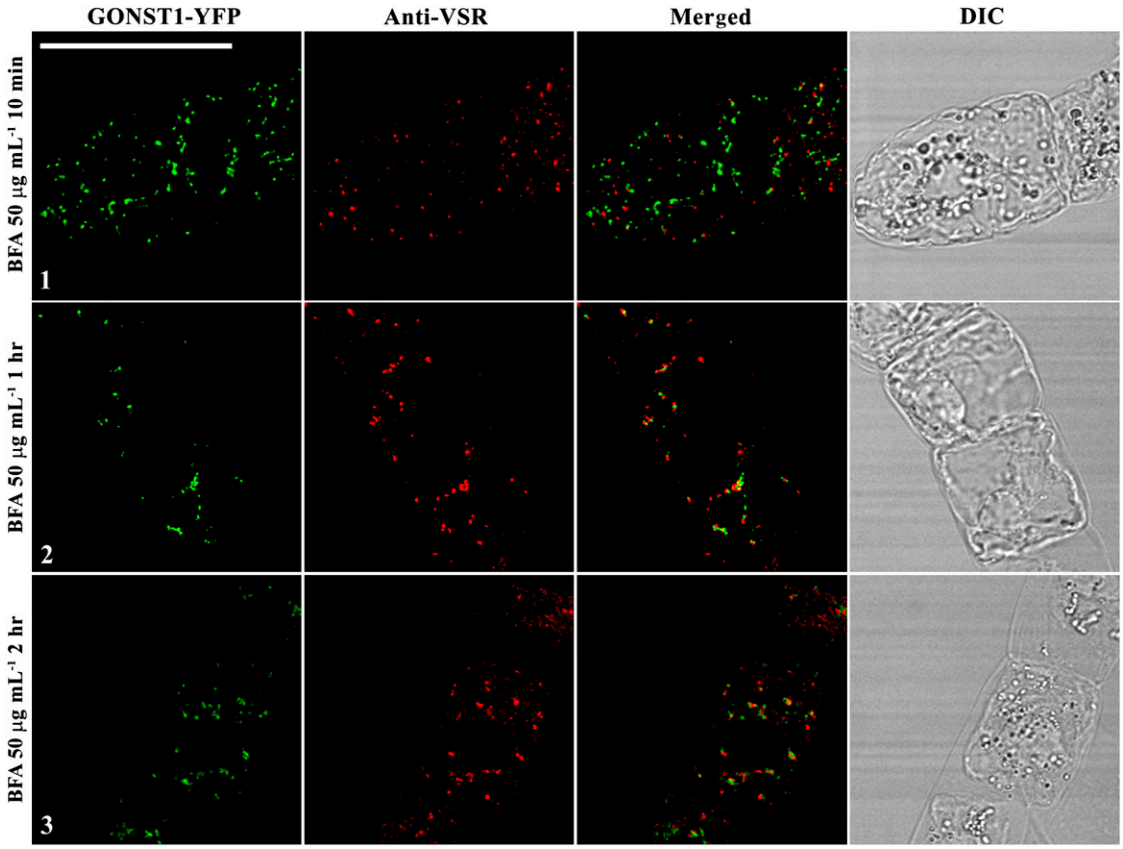

Figure 6. Formation of Golgi-PVC hybrids was time dependent. Transgenic BY-2 cells expressing the Golgi reporter GONST1-YFP were treated with BFA at 50 μg mL^{-1}, followed by sample collection at indicated time points and used for fixation. The fixed cells were then labeled with VSR antibodies to detect PVCs (red), whereas the YFP-marked Golgi (green) was ready for detection. DIC images show the morphology of the tested cells. Bar = 50 μm.

To study further the details of these Golgi- or PVC-derived aggregates in response to BFA treatment, we then performed structural transmission electron microscopy (TEM) studies using conventional chemical fixation and subsequent embedding in Spurr's resin as previously described (Tse et al., 2004). First, day 3 transgenic GONST1-YFP BY-2 cells were treated with BFA at 0, 10 (controls), and 100 μg mL^{-1} for 1 h. Cells were then prepared for TEM analysis as described (Tse et al., 2004). As shown in Supplemental Figure S5, in untreated control cells, normal Golgi apparatus (A) and typical multivesicular PVCs (B) were detected. In addition, in cells treated with a low concentration of BFA (at 10 μg mL^{-1}), typical BFA-induced Golgi aggregates with visible ER-Golgi hybrids (C) were observed, whereas normal multivesicular PVCs remained unchanged in size and morphology (D). However, in cells treated with BFA at 100 μg mL^{-1}, many aggregated vesicles with sizes of 100 to 200 nm, but lacking internal vesicular structures, were often observed in these BFA-treated cells (Fig. 9A), a result consistent with the immunoEM study in which aggregated vesicles were found to be labeled by VSR antibodies in BFA-treated cells (Fig. 8, E–H). Such detection was due to BFA treatment because no such aggregated vesicles around the Golgi apparatus were observed in untreated cells (data not shown). Thus, these aggregated vesicles may represent BFA-induced aggregates derived from PVCs in BY-2 cells. Similar vesicle aggregates were also observed from Arabidopsis root-tip cells treated with BFA at 100 μg mL^{-1} for 1 h (Fig. 9B), indicating that such BFA effect on PVC is not limited to tobacco BY-2 cells.

BFA Induced VSR-Marked PVCs to Form Aggregates in Root-Tip Cells of Other Plants

We have thus far demonstrated that BFA at high concentrations induced both Golgi and PVC to form aggregates in tobacco BY-2 cells and that aggregates derived from Golgi and PVC remained distinct, but closely associated. To find out whether such a BFA response is unique to BY-2 cells or can also be observed in other cell types, we performed additional BFA induction experiments using root-tip cells of various plants. Mature seeds of mung bean, pea, Arabidopsis, and transgenic tobacco expressing the Golgi marker GONST1-YFP were first germinated before the root tips were treated with BFA at 0, 10, and 100 μg mL^{-1} for 1 h, followed by fixation and immunolabeling with VSR

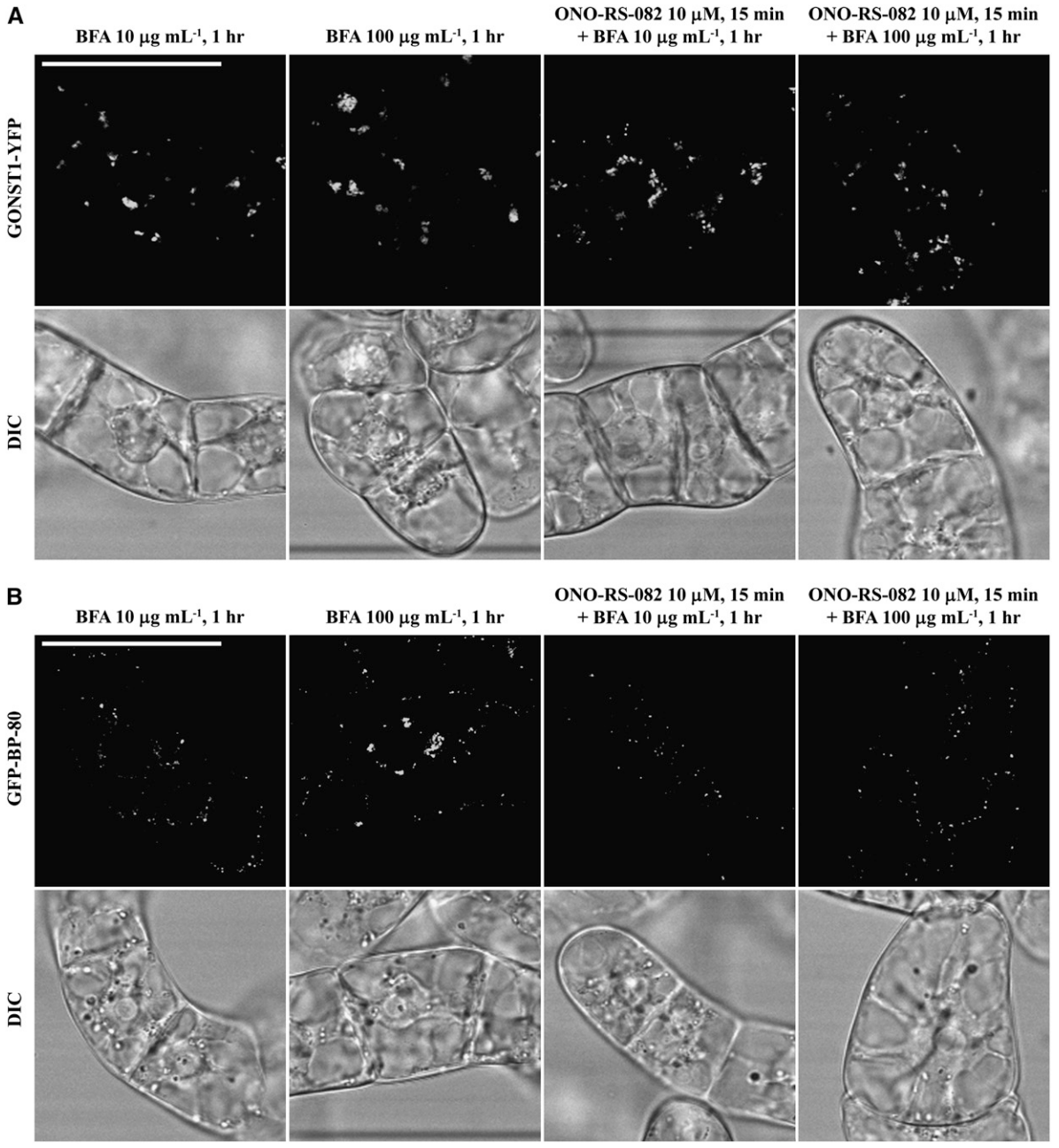

Figure 7. The target of BFA effect on Golgi and PVC is distinct. Transgenic BY-2 cells expressing the Golgi reporter GONST1-YFP (A) and PVC reporter GFP BP-80 (B) were treated with ONO-RS-082 at 10 μM for 15 min, followed by BFA treatment at 10 or 100 μg mL^{-1} for 1 h as indicated (images 3 and 4) before confocal imaging. Controls included BFA treatment at 10 or 100 μg mL^{-1} for 1 h before confocal imaging (images 1 and 2). DIC images show the morphology of the tested cells. Bars = 50 μm.

antibodies. As shown in Figure 10, typical punctate patterns were observed in tobacco root-tip cells expressing the Golgi marker GONST1-YFP, and these YFP-marked Golgi formed aggregates in the presence of BFA at either 10 or 100 μg mL^{-1} (Fig. 10, column 1), a result consistent with that observed in transgenic GONST1-YFP BY-2 cells. These results indicated that BFA at high concentrations induced the Golgi to form aggregates in tobacco root-tip cells. In contrast, BFA at low concentrations (0 or 10 μg mL^{-1}) did not induce any changes in the VSR-marked PVCs, but BFA at high concentrations (100 μg mL^{-1}) induced the VSR-marked PVCs to form aggregates in root-tip cells of mung bean, pea, and Arabidopsis (Fig. 10, columns 2–4). Moreover, PVC-derived aggregates in Arabidopsis root-tip cells (Fig. 9B) look similar to those in BY-2 cells (Fig. 9A). Therefore, BFA at high concentrations induced Golgi and PVC to form aggregates in root-tip cells of various plants in a way that is similar to that of BY-2 cells.

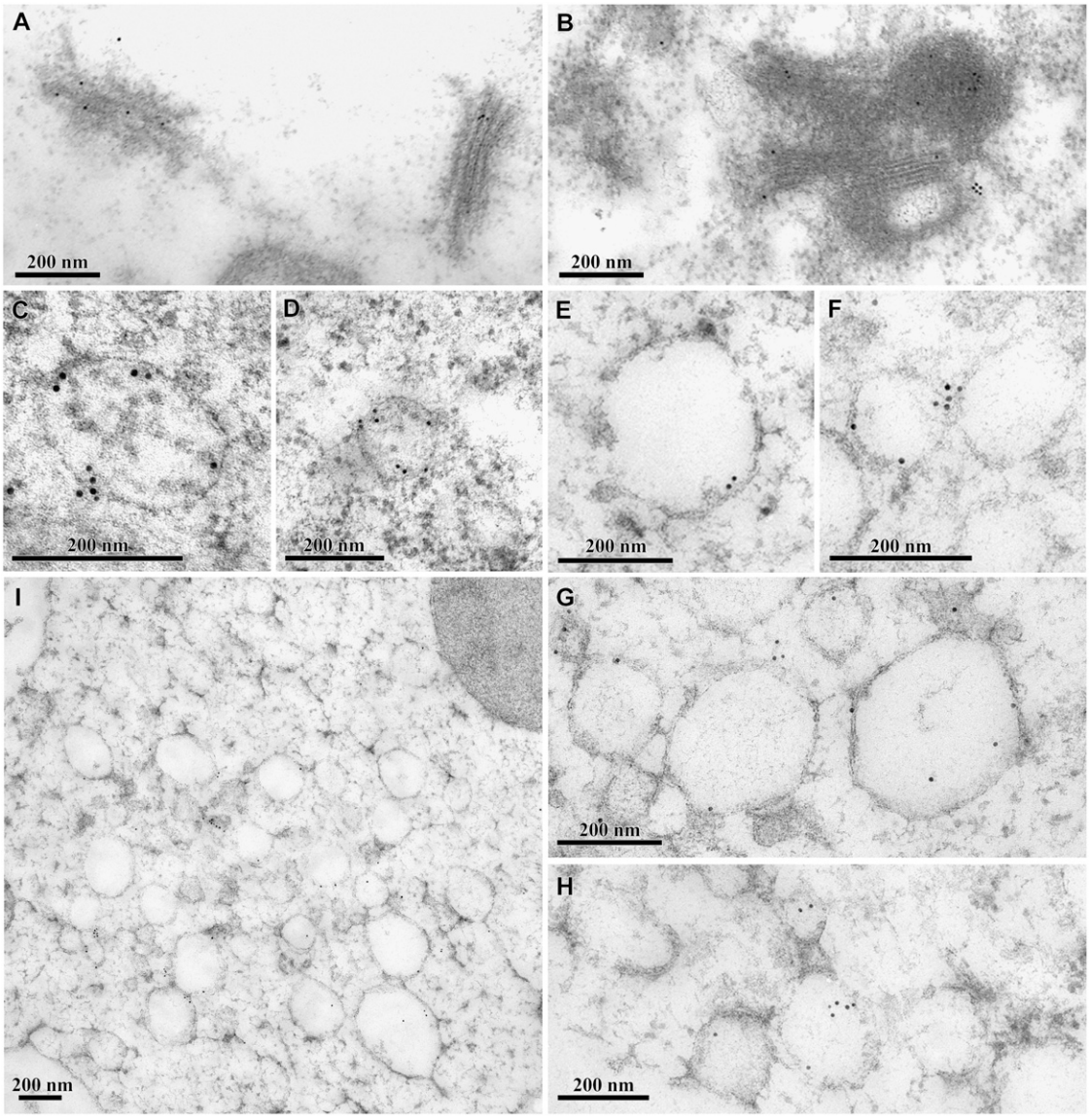

Figure 8. ImmunoEM identification of BFA-induced aggregates derived from Golgi and PVC. A, GFP antibodies labeled the Golgi stacks in untreated transgenic GONST1-YFP cells using ultrathin sections of Lowicryl (HM20). B, GFP antibodies labeled the curved Golgi structures in transgenic GONST1-YFP cells treated with BFA at 100 μg mL^{-1}, using ultrathin sections of Lowicryl (HM20). C and D, Multivesicular PVCs as detected by VSR antibodies in untreated cells using ultrathin sections from high-pressure frozen/freeze-substituted material. E to H, PVC or PVC aggregates as detected by VSR antibodies in cells treated with BFA at 100 μg mL^{-1}, using ultrathin samples of high-pressure frozen/freeze-substituted material. Bars = 200 nm. I, Overview of BFA-induced PVC aggregates in BY-2 cells treated with BFA at 100 μg mL^{-1} for 1 h, followed by high-pressure frozen/freeze substituted material. Bars = 500 nm.

DISCUSSION

Transgenic BY-2 Cells Expressing the PVC Reporter Are Useful Tools for Studying the Dynamics of PVCs

Transgenic tobacco BY-2 cells expressing GFP-tagged organelle markers have been useful tools for studying the dynamics of various endomembrane organelles, including ER and Golgi apparatus (Satiat-Jeunemaitre et al., 1999). Prevacuolar/endosomal compartments are important organelles that mediate protein trafficking in the secretory and endocytic pathways of eukaryotic cells. Several proteins have been used as markers to define PVCs in plant cells, including syntaxin (Bassham et al., 1995; Conceicao et al., 1997), small GTPase (Ueda et al., 2004), and VSR proteins (Li et al., 2002; Tse et al., 2004; Lam et al., 2005). More recently, we have generated transgenic tobacco BY-2 cell lines expressing the YFP BP-80 reporter for PVCs. Using VSR antibodies and the YFP BP-80 reporter expressing transgenic tobacco BY-2 cells as markers, PVCs were identified as mobile MVBs in tobacco BY-2 cells (Tse et al., 2004). In this

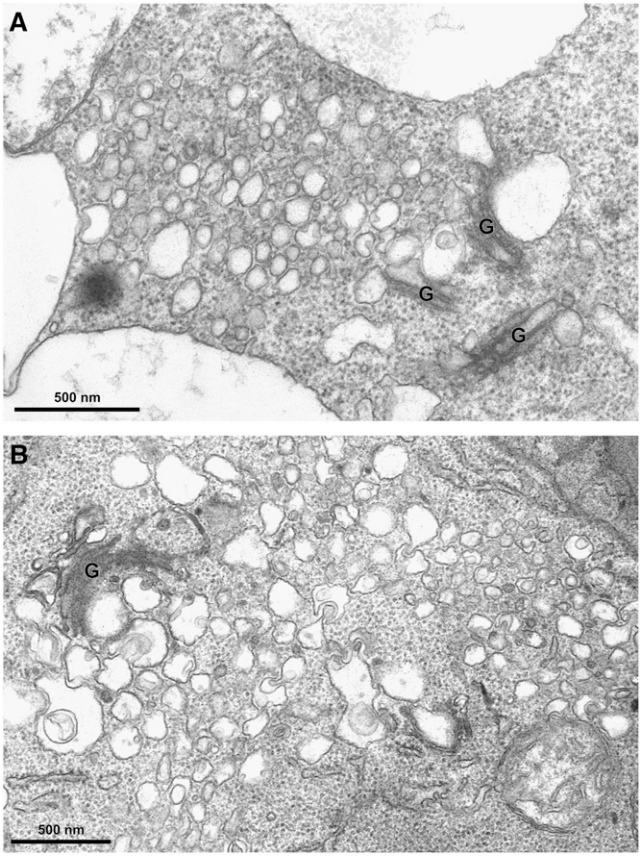

Figure 9. Ultrastructural analysis of BFA-treated transgenic GONST1-YFP cells and Arabidopsis root-tip cells. A, Overview of BFA-induced Golgi and PVC aggregates in BY-2 cells treated with BFA at 100 μg mL^{-1} for 1 h. B, Overview of BFA-induced Golgi and PVC aggregates in Arabidopsis root tips treated with at BFA at 100 μg mL^{-1} for 1 h. Bars = 200 nm.

study, we used two transgenic BY-2 cells lines expressing either the Golgi marker GONST1-YFP reporter or the PVC marker GFP/YFP BP-80 reporter (Tse et al., 2004) to study the effects of BFA on PVCs in living cells by following changes of fluorescent signals upon drug treatment. We demonstrated that PVCs and Golgi apparatus showed different sensitivity toward BFA treatments where BFA at physiologically high concentrations induced PVCs to form aggregates that remained distinct from Golgi-derived BFA-induced aggregates.

PVCs and Golgi Have Different Sensitivity to BFA Treatment in BY-2 Cells

The Golgi apparatus provides a site for rapid action in both mammalian and plant cells where BFA induces Golgi to form an ER-Golgi hybrid or a BFA compartment. However, mammalian cells and plant cells have different sensitivity to BFA treatment. For example, BFA at 2.8 μg mL^{-1} was sufficient and specific to induce the formation of BFA compartments and block protein traffic from ER to Golgi in animal cells (Klausner et al., 1992), but a higher concentration of BFA (i.e. at 10 μg mL^{-1}) was required to induce Golgi changes (Satiat-Jeunemaitre and Hawes, 1992; Driouich et al., 1993) and block ER-to-Golgi protein traffic (Jiang and Rogers, 1998) in plant cells. However, BFA at 10 μg mL^{-1} did not cause detectable morphological changes for PVCs in BY-2 cells (Tse et al., 2004). Therefore, the fate of Golgi apparatus in BFA-treated BY-2 cells is affected by BFA in a concentration-dependent manner. These results are consistent with previous studies in maize (*Zea mays*) root cells (Satiat-Jeunemaitre et al., 1996) and in tobacco BY-2 cells (Nebenfuhr et al., 2002; Ritzenthaler et al., 2002).

In addition to ER and Golgi apparatus, BFA may also act on endosomes in mammalian cells. For example, BFA treatment induced endosomes to become tubulated in mammalian cells (Hunziker et al., 1991; Lippincott-Schwartz et al., 1991; Wood et al., 1991), which may be due to the involvement of Arf1 in the formation of transport vesicles between early and late endosomes in mammalian cells (Gu and Gruenberg, 2000). Furthermore, BFA treatment caused changes in the membrane composition of endosomes in mammalian cells and yeast (*Saccharomyces cerevisiae*; Donaldson and Jackson, 2000).

In this study, we extended our understating to BFA effects on the prevacuolar organelles using transgenic tobacco BY-2 cells expressing the PVC marker GFP BP-80 reporter. We demonstrated that PVCs/MVBs in BY-2 cells formed aggregates in response to BFA treatment at high concentrations (i.e. at 50–100 μg mL^{-1}), but not at low concentrations (i.e. at 5–10 μg mL^{-1}). Such high BFA concentrations were within reversible levels because the tested organelles recovered fully (based on the punctate fluorescent patterns) when the drug was washed off. Furthermore, the target of the BFA effect on Golgi and PVC is distinct because the phospholipase A_2 inhibitor ONO-RS-082 specifically prevented PVCs, but not Golgi, from forming aggregates in the presence of BFA. Furthermore, the delayed observation of PVC-derived aggregates compared to Golgi-derived aggregates indicated that the Golgi apparatus might be more sensitive than PVC in response to BFA treatment, which might be due to the different ADP-ribosylation factor (ARF) GEFs (exchange factors for ARF GTPases) present in these two organelles (Geldner et al., 2003). However, it is not clear whether the BFA-induced PVC response is a consequence of the Golgi response or whether the effect of BFA on Golgi and PVC is independent of each other.

In addition, PVC-derived aggregates as identified by VSR antibodies in confocal immunofluorescence remained distinct from Golgi-derived aggregates in the same BFA-treated cells. ImmunoEM and structural TEM studies further identified PVC-derived aggregates as clusters of VSR-labeled PVCs with similar size (about 100–200 nm in diameter), but lost the appearance of their internal vesicles. Such BFA effect on PVCs in BY-2 cells is different from the effect of wortmannin on PVCs in which wortmannin induced PVCs to form small vacuoles, but the enlarged vacuoles still contain visible, but reduced, internal vesicles (Tse et al., 2004).

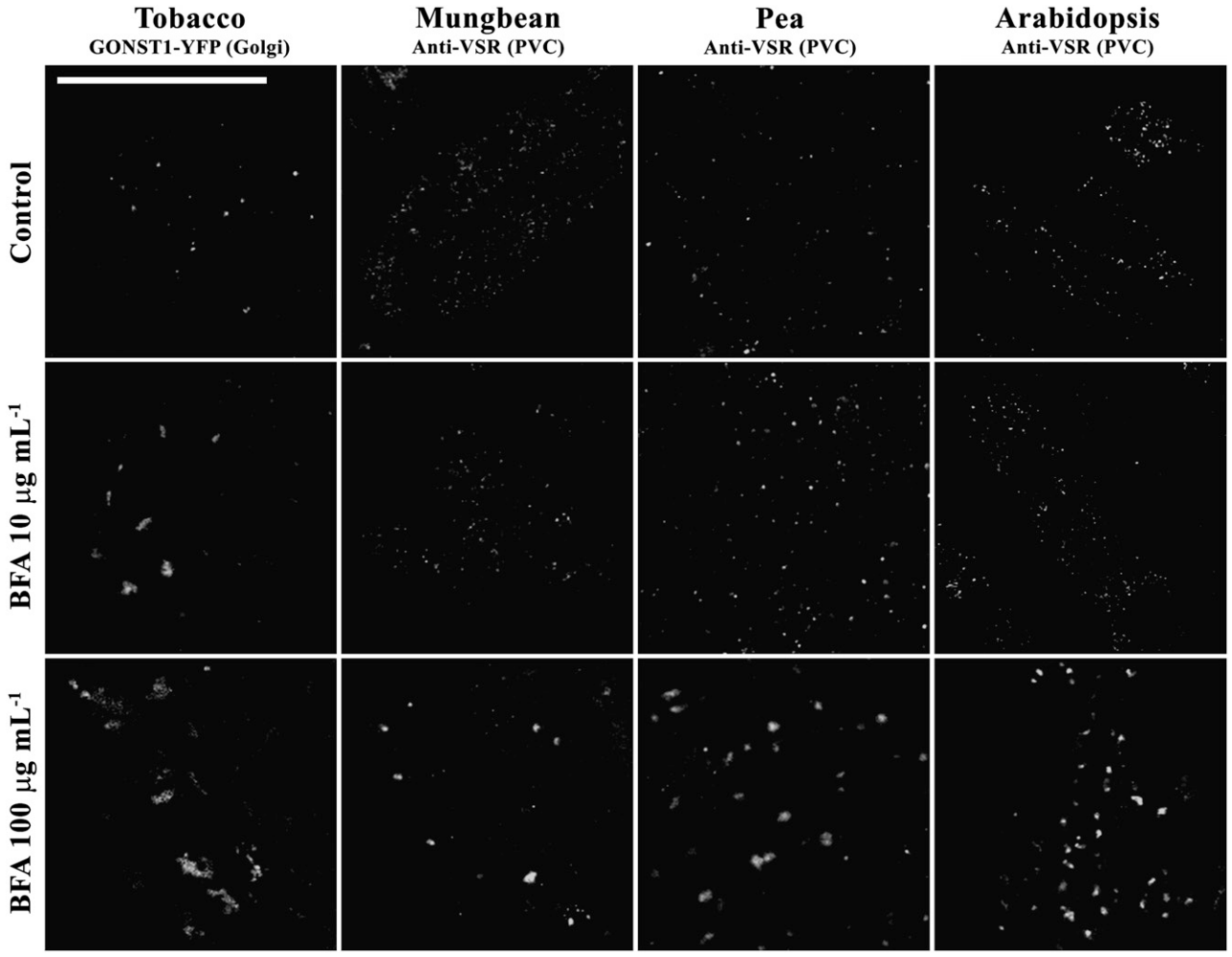

Figure 10. BFA also induced VSR-marked PVCs to form aggregates in other plant cell types. Root-tip cells from germinating seeds of transgenic GONST1-YFP tobacco, mung bean, pea, and Arabidopsis were treated with BFA at 0, 10, and 100 μg mL^{-1} for 1 h as indicated before they were either used for direct confocal imaging (for tobacco cells) to ready detect Golgi apparatus, or fixed and labeled with VSR antibodies (for pea, mung bean, and Arabidopsis root-tip cells) to detect PVCs. Bar = 50 μm.

In addition, BFA-induced PVC-derived aggregates were not limited to BY-2 cells, but also observed in several other cell types, including root-tip cells of pea, tobacco, rice (*Oryza sativa*), and Arabidopsis. Therefore, it seems that the BFA effect on PVCs is a general response in plant cells. It is thus interesting and important to find out the possible physiological consequences of PVC changes in response to BFA treatment and the molecular mechanism of BFA action on plant PVCs.

PVCs and Endosomes May Have Different Sensitivity to BFA in Plant Cells

In this study, we have shown that Golgi and PVC have different sensitivity to BFA, where BFA at low concentrations (5–10 μg mL^{-1}) caused Golgi, but not PVC, to form aggregates, whereas high BFA concentrations (50–100 μg mL^{-1}) induced both Golgi and PVC to form aggregates. Several recent studies also demonstrated that BFA induced endosomes to form aggregates in plant cells. The Arabidopsis GNOM protein (an exchange factor for ARF GTPases-ARF-GEFs), which plays an important role in mediating endosomal recycling, auxin transport, and plant growth in Arabidopsis, was found to locate to endosomes because this protein colocalized with the internalized FM4-64 endosomal marker 30 min after the uptake study (Geldner et al., 2003). When Arabidopsis root-tip cells were treated with BFA at 14 μg mL^{-1} (50 μM), the GNOM-marked endosomal compartments formed aggregates (Geldner et al., 2003). However, these GNOM-marked endosomal compartments might be different from the PVCs marked by GFP BP-80 in transgenic BY-2 cells in this study. First, the PVCs marked by the GFP BP-80 reporter did not form aggregates when transgenic BY-2 cells were treated with BFA at 10 μg/mL (Tse et al., 2004), a concentration that induced GNOM-marked endosomes to form aggregates in Arabidopsis cells (Geldner et al., 2003). Second, VSR-marked PVCs were identified as MVBs in

BY-2 cells; such multivesicular nature is consistent with the identity of late endosomes (Tse et al., 2004). Third, 30 min after the uptake study with the endosomal marker FM4-64, PVCs marked by the GFP BP-80 reporter were found to colocalize with the internalized dye (Tse et al., 2004), a similar time required for internalization of FM4-64 to the GNOM-marked endosome in Arabidopsis root-tip cells. However, VSR-marked PVCs in BY-2 cells and the GNOM-marked endosomes might still represent two distinct endocytic compartments because the uptake rate of FM4-64 in BY-2 cells and Arabidopsis root cells might be different. Last, we have recently generated transgenic BY-2 cell lines expressing fusion proteins containing GFP and a rice secretory carrier-associated membrane protein (SCAMP; GFP-SCAMP) that mark both plasma membrane and internalized vesicles, where these GFP-marked vesicles are identified as early endosomes and BFA at low concentrations (5–10 μg mL^{-1}) induced them to form aggregates (Lam et al., 2006). In addition, the different sensitivity of Golgi, PVC, and (early) endosome to BFA might lie in organelle-specific localization of different ARF GEFs, where endosome-specific GNOM determines the sensitivity of PIN1 recycling in Arabidopsis cells (Geldner et al., 2003). Taken together, the VSR-marked PVCs/MVBs might represent late endosomes merging from the endocytic pathway in tobacco BY-2 cells.

BFA-Induced Golgi-Derived Aggregates or ER Patterns

In this study, day 3 or day 2 BY-2 cells after subcultures were used to study the effects of BFA on PVC/MVB in tobacco BY-2 cells mainly for two reasons. First, cells at these 2 d are at their log phase, thus representing physiologically healthy stages, whereas cells at day 6 or day 7 represent stationary stages (Matsuoka et al., 2004). Second, in transgenic BY-2 cells expressing the PVC marker XFP BP-80, typical punctate fluorescent patterns representing PVCs/MVBs (Tse et al. 2004) were observed in day 2 or day 3 cells, but such PVC patterns gradually disappear during later stages of cultures with fluorescent signals detected in vacuoles at day 6 and day 7 cells (Mitsuhashi et al., 2000; Lo and Jiang, 2006).

When day 3 or day 2 GONST1-YFP BY-2 cells were treated with BFA at 10 μg mL^{-1} for 1 h, typical Golgi aggregates were observed (e.g. Fig. 2A). In addition, similar BFA-induced aggregates were also observed in root cells of transgenic tobacco expressing the GONST1-YFP (Fig. 10). Such BFA-induced Golgi aggregations have been documented by many previous studies in various cell types, including Arabidopsis root cells for the expressed mammalian sialytransferase (ST; Wee et al., 1998), tobacco BY-2 cells for GONST1-YFP (Tse et al., 2004; Miao et al., 2006), living onion (*Allium cepa*) epidermal cells for GONST1-YFP (Baldwin et al., 2001), Arabidopsis cotyledon epidermal cells for KAMΔC:mRFP (Kong et al., 2006), maize root cells for JIM84 (Satiat-Jeunemaitre and Hawes, 1992; Satiat-Jeunemaitre et al., 1996), and Arabidopsis root cells for JIM84/ADL6 (Jin et al., 2001). However, several other studies have also demonstrated that BFA induced the reporter-marked Golgi to form ER patterns in various cell types, including tobacco epidermal cells for the STtmd-GFP (Boevink et al., 1998), tobacco BY-2 cells for Man1-GFP (Ritzenthaler et al., 2002), and tobacco leaf epidermal cells and BY-2 cells for ST-GFP (Saint-Jore et al., 2002). Therefore, it seems that there are a variety of responses of tissues and Golgi markers to BFA. Furthermore, different BFA concentrations used and different lengths of BFA treatment time before imaging may also contribute to these observed variations.

In addition, the physiological status of cells may contribute to such variation. Indeed, when day 3 and day 6 GONST1-YFP BY-2 cells were subjected to BFA treatment at 10 μg mL^{-1} for 1 h, aggregation patterns and ER patterns were observed from these two stages of cells, respectively (Supplemental Fig. S2). However, when another BY-2 cell line expressing Man1-GFP was used, ER patterns were observed from both day 3 and day 6 cells after BFA treatment (Supplemental Fig. S2). However, we do not know whether such differences between GONST1-YFP and Man1-GFP BY-2 cell lines are due to the difference between the trans-Golgi localization of GONST1-YFP and the cis-Golgi localization of Man1-GFP, or due to their different sensitivity to BFA treatment, or, even though unlikely, due to the different localization of GONST1-YFP and Man1-GFP to different populations of the Golgi apparatus in BY-2 cells. Because BFA-induced aggregates for GONST1-YFP have been demonstrated by several studies in living onion epidermal cells (Baldwin et al., 2001), tobacco BY-2 cells (Tse et al., 2004; this study), and root cells of transgenic tobacco (this study), it would thus be reasonable to use GONST1-YFP BY-2 cells as a control for the XFP BP-80 BY-2 cells to study the effect of BFA on PVC/MVB in BY-2 cells in this study.

CONCLUSION

Several endomembrane organelles, including the ER and the Golgi, formed aggregates in response to BFA treatment, which also affects the transport of proteins from the ER to the Golgi in the secretory pathway. The development of transgenic tobacco BY-2 cell lines expressing GFP-marked PVCs and the identification of MVBs as PVCs have allowed us to study the dynamic response of PVCs to various drugs in living cells. For example, wortmannin treatment induced GFP-marked PVCs to form small vacuoles and thus provided a quick tool for defining multivesicular PVCs in tobacco BY-2 cells (Tse et al., 2004). In this study, we demonstrated that BFA at high concentrations (50 or 100 μg mL^{-1}) induced both YFP-marked PVCs and Golgi to form typical enlarged aggregates, but the PVC-derived aggregates remained physically distinct from the Golgi-derived aggregates. In addition,

the BFA-induced formation of aggregates derived from PVCs was specifically inhibited by a phospholipase A_2 inhibitor ONO-RS-082, but this drug did not prevent the formation of BFA-induced Golgi-derived aggregates in BY-2 cells. The different changes of Golgi and PVC in response to wortmannin and BFA would provide quick tools to distinguish PVC from Golgi and identify PVC that will serve as a first step to study the molecular mechanism of the BFA effect on PVC-mediated protein traffic in the secretory and endocytic pathways of plant cells. Several questions can be addressed in future research. For example, what is the molecular target of BFA on PVC? Does BFA also affect PVC-mediated protein trafficking between Golgi and PVC or between PVC and plasma membrane? What are the molecular mechanisms of PVC-mediated protein trafficking in the plant secretory pathway? What is the physiological significance of BFA-induced PVC-derived aggregates in plant cells? Our current research is addressing some of these questions to further understand the roles of PVCs in plant cells.

MATERIALS AND METHODS

General methods for construction of recombinant plasmids, characterization of cloned inserts, transformation of tobacco (*Nicotiana tabacum*) BY-2 cells, maintenance of transgenic tobacco BY-2 cells, and preparation and characterization of antibodies have been described previously (Jiang and Rogers, 1998, 2001; Cao et al., 2000; Jiang et al., 2000; Tse et al., 2004). BY-2 cells were maintained by subculture twice a month on agar plates or every 7 d in liquid cultures at room temperature (21°C–22°C). Liquid cultures were kept in shakers at 125 rpm.

Generation of Transgenic BY-2 Cells Expressing the GFP BP-80 Reporter

GFP with a signal peptide sequence from proaleurain (spGFP) was amplified by PCR and subcloned into the pYFP BP-80 construct via *Hin*dIII/*Eco*RI sites to replace the pYFP and resulted in pGFP BP-80 (Tse et al., 2004). The resulting pGFP BP-80 construct was then transformed into the Agrobacterium LBA4404, followed by transforming BY-2 cells as previously described (Tse et al., 2004). In addition, transgenic tobacco plants expressing the Golgi marker GONST1-YFP and the PVC reporter pYFP-BP-80 were generated via Agrobacterium-mediated transformation as previously described (Jiang et al., 2000).

BFA Treatment and Recovery Studies

For BFA treatment experiments, aliquots of BFA (stock at 2.5 mg mL^{-1} in dimethyl sulfoxide) solution were added to 2- and 3-d-old suspension cultures (log phase cultures) to give the proper final concentrations. BFA-treated cells were then removed from the cultures at indicated times for direct confocal imaging or fixed for confocal immunofluorescence and EM. For recovery experiments, BY-2 cells were treated with BFA at indicated concentrations, followed by centrifugations at low speed and washing three times with fresh Murashige and Skoog medium before samples were used for confocal imaging or fixation. On average, more than 100 cells were observed to obtain similar results for each experiment. All drug treatment experiments had been repeated at least two to three times with similar results to make sure that the drugs were functional and the cells used were at the same or similar physiological stages.

ONO-RS-082 and BEL Treatment

For drug treatment using OBO-RS-082 (BIOMOL) and BEL (Sigma), aliquots of the ONO-RS-082 and BEL (stock at 1 mM in dimethyl sulfoxide) solution were added to 2- to-3-d-old suspension cultures to give the proper final concentrations and incubated for 15 min, followed by addition of BFA at indicated final concentrations and incubated for 1 h. The treated cells were then collected and subjected to direct confocal imaging.

Antibodies

Production and characterization of VSR antibodies were described previously (Tse et al., 2004). Secondary lissamine rhodamine-conjugated affinity-purified anti-rabbit antibodies were purchased from Jackson ImmunoResearch Laboratories.

Confocal Immunofluorescence Studies

Fixation and preparation of tobacco BY-2 cells, labeling, and analysis by epifluorescence and confocal immunofluorescence have been described previously (Jiang and Rogers, 1998; Jiang et al., 2000; Li et al., 2002). The parameters for collecting confocal images within the linear range were settled as previously described (Jiang and Rogers, 1998). For single labeling, 4 μg mL^{-1} of polyclonal rabbit VSR antibodies were incubated at 4°C overnight. All confocal fluorescence images were collected using a Bio-Rad Radiance 2100 system. Images were processed using Adobe Photoshop software as previously described (Jiang and Rogers, 1998).

EM of Resin-Embedded Cells

For samples embedded in LR White and Lowicryl (HM20) for immunoEM studies, cells were fixed in 1 mL of a primary fixative solution containing 0.25% (v/v) glutaraldehyde and 1.5% (v/w) paraformaldehyde in 50 mM phosphate buffer, pH 7.4, for 15 min at room temperature and then transferred to 4°C for an additional 16 h. After washing with phosphate buffer at room temperature, cells were dehydrated in an ethanol series and then embedded in LR White and Lowicryl (HM20) resin.

For samples embedded in Spurr's resin for structural TEM studies, cells were fixed in 1 mL of a primary fixative containing 2% (v/v) glutaraldehyde and 0.1 mL of saturated picric acid in 25 mM CaCo buffer, pH 7.2, for 15 min at room temperature and then transferred to 4°C for an additional 16 h. After washing with 25 mM CaCo buffer, pH 7.2, cells were further subjected to a secondary fixative solution containing 2% (w/v) osmium tetroxide and 0.5% (w/v) potassium ferrocyanide in 25 mM CaCo buffer, pH 7.2, for 2 h at room temperature. The cells were then washed with 25 mM CaCo buffer, pH 7.2, followed by contrasting at 2% aqueous uranyl acetate for 2 h at room temperature. After washing twice in water, cells were dehydrated in an acetone series and finally embedded in Spurr's resin.

For sample preparation using high-pressure frozen/freeze substituted, procedures were performed essentially as described previously (Tse et al., 2004). Ultrathin sections were then prepared from these blocks and used in either immunoEM or structural TEM studies as described (Tse et al., 2004). VSR and GFP antibodies (at 40 μg mL^{-1} diluted with phosphate-buffered saline containing 1% bovine serum albumin) were used in immunoEM studies.

Supplemental Data

The following materials are available in the online version of this article.

Supplemental Figure S1. BFA induces YFP-marked PVCs to form aggregates in a dose-dependent manner.

Supplemental Figure S2. Formation of BFA-induced Golgi aggregates in GONST1-YFP cells is stage dependent.

Supplemental Figure S3. Recovery of BFA-induced aggregates.

Supplemental Figure S4. Target of BFA effect on Golgi and PVC is distinct.

Supplemental Figure S5. Ultrastructural analysis of BFA-treated transgenic GONST1-YFP cells.

ACKNOWLEDGMENTS

We are grateful to Prof. David G. Robinson (University of Heidelberg) and John C. Rogers (National Science Foundation) for their continuous support of our studies. A portion of this work has been presented in abstract form for a poster for the American Society of Plant Biologists Annual Meeting 2005 (http://abstracts.aspb.org/pb2005/public/P51/7276.html).

Received September 27, 2006; accepted October 9, 2006; published October 13, 2006.

LITERATURE CITED

Baldwin TC, Handford MG, Yuseff MI, Orellana A, Dupree P (2001) Identification and characterization of GONST1, a Golgi-localized GDP-mannose transporter in Arabidopsis. Plant Cell **13:** 2283–2295

Bassham DC, Gal S, daSilva CA, Raikhel NV (1995) An Arabidopsis syntaxin homologue isolated by functional complementation of a yeast pep12 mutant. Proc Natl Acad Sci USA **92:** 7262–7266

Bethke PC, Jones RL (2000) Vacuoles and prevacuolar compartments. Curr Opin Plant Biol **3:** 469–475

Boevink P, Oparka K, Santa CS, Martin B, Betteridge A, Hawes C (1998) Stacks on tracks: the plant Golgi apparatus traffics on an actin/ER network. Plant J **15:** 441–447

Bright NA, Lindsay MR, Stewart A, Luzio JP (2001) The relationship between lumenal and limiting membranes in swollen late endocytic compartments formed after wortmannin treatment or sucrose accumulation. Traffic **2:** 631–642

Busch M, Mayer U, Jurgens G (1996) Molecular analysis of the Arabidopsis pattern formation of gene GNOM: gene structure and intragenic complementation. Mol Gen Genet **250:** 681–691

Cao X, Rogers SW, Butler J, Beevers L, Rogers JC (2000) Structural requirements for ligand binding by a probable plant vacuolar sorting receptor. Plant Cell **12:** 493–506

Conceicao AS, Marty-Mazars D, Bassham DC, Sanderfoot AA, Marty F, Raikhel NV (1997) The syntaxin homolog AtPEP12p resides on a late post-Golgi compartment in plants. Plant Cell **9:** 571–582

daSilva LL, Taylor JP, Hadlington JL, Hanton SL, Snowden CJ, Fox SJ, Foresti O, Brandizzi F, Denecke J (2005) Receptor salvage from the prevacuolar compartment is essential for efficient vacuolar protein targeting. Plant Cell **17:** 132–148

de Figueiredo P, Drecktrah D, Katzenellenbogen JA, Strang M, Brown WJ (1998) Evidence that phospholipase A2 activity is required for Golgi complex and trans Golgi network membrane tubulation. Proc Natl Acad Sci USA **95:** 8642–8647

de Figueiredo P, Polizotto RS, Drecktrah D, Brown WJ (1999) Membrane tubule-mediated reassembly and maintenance of the Golgi complex is disrupted by phospholipase A2 antagonists. Mol Biol Cell **10:** 1763–1782

Dettmer J, Hong-Hermesdorf A, Stierhof YD, Schumacher K (2006) Vacuolar H+-ATPase activity is required for endocytic and secretory trafficking in Arabidopsis. Plant Cell **18:** 715–730

Donaldson JG, Jackson CL (2000) Regulators and effectors of the ARF GTPases. Curr Opin Cell Biol **12:** 475–482

Driouich A, Zhang GF, Staehelin LA (1993) Effect of brefeldin A on the structure of the Golgi apparatus and on the synthesis and secretion of proteins and polysaccharides in sycamore maple (*Acer pseudoplatanus*) suspension-cultured cells. Plant Physiol **101:** 1363–1373

Geldner N, Anders N, Wolters H, Keicher J, Kornberger W, Muller P, Delbarre A, Ueda T, Nakano A, Jurgens G (2003) The Arabidopsis GNOM ARF-GEF mediates endosomal recycling, auxin transport, and auxin-dependent plant growth. Cell **112:** 219–230

Grebe M, Xu J, Mobius W, Ueda T, Nakano A, Geuze HJ, Rook MB, Scheres B (2003) Arabidopsis sterol endocytosis involves actin-mediated trafficking via ARA6-positive early endosomes. Curr Biol **13:** 1378–1387

Griffiths G, Matteoni R, Back R, Hoflack B (1990) Characterization of the cation-independent mannose 6-phosphate receptor-enriched prelysosomal compartment in NRK cells. J Cell Sci **95:** 441–461

Gu F, Gruenberg J (2000) ARF1 regulates pH-dependent COP functions in the early endocytic pathway. J Biol Chem **275:** 8154–8160

Hess MW, Muller M, Debbage PL, Vetterlein M, Pavelka M (2000) Cryopreparation provides new insight into the effects of brefeldin A on the structure of the HepG2 Golgi apparatus. J Struct Biol **130:** 63–72

Hunziker W, Whitney JA, Mellman I (1991) Selective inhibition of transcytosis by brefeldin A in MDCK cells. Cell **67:** 617–627

Jackson CL, Casanova JE (2000) Turning on ARF: the Sec7 family of guanine-nucleotide-exchange factors. Trends Cell Biol **10:** 60–67

Jiang L, Phillips TE, Rogers SW, Rogers JC (2000) Biogenesis of the protein storage vacuole crystalloid. J Cell Biol **150:** 755–770

Jiang L, Rogers JC (1998) Integral membrane protein sorting to vacuoles in plant cells: evidence for two pathways. J Cell Biol **143:** 1183–1199

Jiang L, Rogers JC (2001) Compartmentation of proteins in the protein storage vacuole: a compound organelle in plant cells. Adv Bot Res **35:** 139–173

Jiang L, Rogers JC (2003) Sorting of lytic enzymes in the plant Golgi apparatus. Annu Plant Rev **9:** 114–140

Jin JB, Kim YA, Kim SJ, Lee SH, Kim DH, Cheong GW, Hwang I (2001) A new dynamin-like protein, ADL6, is involved in trafficking from the trans-Golgi network to the central vacuole in Arabidopsis. Plant Cell **13:** 1511–1526

Katzmann DJ, Odorizzi G, Emr SD (2002) Receptor downregulation and multivesicular-body sorting. Nat Rev Mol Cell Biol **3:** 893–905

Klausner RD, Donaldson JG, Lippincott-Schwartz J (1992) Brefeldin A: insights into the control of membrane traffic and organelle structure. J Cell Biol **116:** 1071–1080

Kobayashi T, Stang E, Fang KS, de Moerloose P, Parton RG, Gruenberg J (1998) A lipid associated with the antiphospholipid syndrome regulates endosome structure and function. Nature **392:** 193–197

Kong SG, Suzuki T, Tamura K, Mochizuki N, Hara-Nishimura I, Nagatani A (2006) Blue light-induced association of phototropin 2 with the Golgi apparatus. Plant J **45:** 994–1005

Lam SK, Siu CL, Hillmer S, Jang S, An G, Robinson DG, Jiang L (2006) SCAMPs define clathrin-coated, trans Golgi-located tubular vesicular structures as an early endosome in tobacco BY-2 cells. Plant Cell (in press)

Lam SK, Tse YC, Jiang L, Oliviusson P, Heinzerling O, Robinson DG (2005) Plant prevacuolar compartments and endocytosis. Plant Cell Monogr **1:** 37–61

Lemmon SK, Traub LM (2000) Sorting in the endosomal system in yeast and animal cells. Curr Opin Cell Biol **12:** 457–466

Li YB, Rogers SW, Tse YC, Lo SW, Sun SS, Jauh GY, Jiang L (2002) BP-80 and homologs are concentrated on post-Golgi, probable lytic prevacuolar compartments. Plant Cell Physiol **43:** 726–742

Lippincott-Schwartz J, Yuan L, Tipper C, Amherdt M, Orci L, Klausner RD (1991) Brefeldin A's effects on endosomes, lysosomes, and the TGN suggest a general mechanism for regulating organelle structure and membrane traffic. Cell **67:** 601–616

Lo SW, Jiang L (2006) Molecular study of prevacuolar compartments in tobacco BY-2 cells. Biotechnol Agric For **58:** 153–166

Luzio JP, Rous BA, Bright NA, Pryor PR, Mullock BM, Piper RC (2000) Lysosome-endosome fusion and lysosome biogenesis. J Cell Sci **113:** 1515–1524

Matsuoka K, Demura T, Galis I, Horiguchi T, Sasaki M, Tashiro G, Fukuda H (2004) A comprehensive gene expression analysis toward the understanding of growth and differentiation of tobacco BY-2 cells. Plant Cell Physiol **45:** 1280–1289

Maxfield FR, McGraw TE (2004) Endocytic recycling. Nat Rev Mol Cell Biol **5:** 121–132

Miao Y, Yan PK, Kim Y, Hwang I, Jiang L (2006) Localization of green fluorescent protein fusions with the seven Arabidopsis vacuolar sorting receptors to prevacuolar compartments in tobacco BY-2 cells. Plant Physiol (in press)

Mitsuhashi N, Shimada T, Mano S, Nishimura M, Hara-Nishimura I (2000) Characterization of organelles in the vacuolar-sorting pathway by visualization with GFP in tobacco BY-2 cells. Plant Cell Physiol **41:** 993–1001

Nebenfuhr A, Ritzenthaler C, Robinson DG (2002) Brefeldin A: deciphering an enigmatic inhibitor of secretion. Plant Physiol **130:** 1102–1108

Paris N, Rogers SW, Jiang L, Kirsch T, Beevers L, Phillips TE, Rogers JC (1997) Molecular cloning and further characterization of a probable plant vacuolar sorting receptor. Plant Physiol **115:** 29–39

Parton RG, Schrotz P, Bucci C, Gruenberg J (1992) Plasticity of early endosomes. J Cell Sci **103:** 335–348

Raposo G, Tenza D, Murphy DM, Berson JF, Marks MS (2001) Distinct protein sorting and localization to premelanosomes, melanosomes, and lysosomes in pigmented melanocytic cells. J Cell Biol **152:** 809–824

Ritzenthaler C, Nebenfuhr A, Movafeghi A, Stussi-Garaud C, Behnia L, Pimpl P, Staehelin LA, Robinson DG (2002) Reevaluation of the effects of brefeldin A on plant cells using tobacco Bright Yellow 2 cells expressing Golgi-targeted green fluorescent protein and COPI antisera. Plant Cell **14:** 237–261

Robinson DG, Rogers JC, Hinz G (2000) Post-Golgi, prevacuolar compartments. Annu Plant Rev **5:** 270–298

Sachse M, Urbe S, Oorschot V, Strous GJ, Klumperman J (2002) Bilayered clathrin coats on endosomal vacuoles are involved in protein sorting toward lysosomes. Mol Biol Cell **13:** 1313–1328

Saint-Jore CM, Evins J, Batoko H, Brandizzi F, Moore I, Hawes C (2002) Redistribution of membrane proteins between the Golgi apparatus and

endoplasmic reticulum in plants is reversible and not dependent on cytoskeletal networks. Plant J **29:** 661–678

Satiat-Jeunemaitre B, Boevink P, Hawes C (1999) Membrane trafficking in higher plant cells: GFP and antibodies, partners for probing the secretory pathway. Biochimie **81:** 597–605

Satiat-Jeunemaitre B, Cole L, Bourett T, Howard R, Hawes C (1996) Brefeldin A effects in plant and fungal cells: something new about vesicle trafficking? J Microsc **181:** 162–177

Satiat-Jeunemaitre B, Hawes C (1992) Redistribution of a Golgi glycoprotein in plant cells treated with Brefeldin A. J Cell Sci **103:** 1153–1166

Sciaky N, Presley J, Smith C, Zaal KJ, Cole N, Moreira JE, Terasaki M, Siggia E, Lippincott-Schwartz J (1997) Golgi tubule traffic and the effects of brefeldin A visualized in living cells. J Cell Biol **139:** 1137–1155

Tse YC, Mo B, Hillmer S, Zhao M, Lo SW, Robinson DG, Jiang L (2004) Identification of multivesicular bodies as prevacuolar compartments in *Nicotiana tabacum* BY-2 cells. Plant Cell **16:** 672–693

Ueda T, Uemura T, Sato MH, Nakano A (2004) Functional differentiation of endosomes in Arabidopsis cells. Plant J **40:** 783–789

van Dam EM, Stoorvogel W (2002) Dynamin-dependent transferrin receptor recycling by endosome-derived clathrin-coated vesicles. Mol Biol Cell **13:** 169–182

Wee EG, Sherrier DJ, Prime TA, Dupree P (1998) Targeting of active sialyltransferase to the plant Golgi apparatus. Plant Cell **10:** 1759–1768

Wood SA, Park JE, Brown WJ (1991) Brefeldin A causes a microtubule-mediated fusion of the trans-Golgi network and early endosomes. Cell **67:** 591–600